

A new algorithm for Reverse Monte Carlo simulations

Fernando Lus B. da Silva, Bo Svensson, Torbjörn Åkesson, and Bo Jönsson

Citation: *The Journal of Chemical Physics* **109**, 2624 (1998); doi: 10.1063/1.476861

View online: <http://dx.doi.org/10.1063/1.476861>

View Table of Contents: <http://scitation.aip.org/content/aip/journal/jcp/109/7?ver=pdfcov>

Published by the [AIP Publishing](#)



Re-register for Table of Content Alerts

Create a profile.



Sign up today!



A new algorithm for Reverse Monte Carlo simulations

Fernando Luís B. da Silva,^{a)} Bo Svensson, Torbjörn Åkesson, and Bo Jönsson
Physical Chemistry II, Chemical Centre, P.O. Box 124, Lund University, S-221 00 Lund, Sweden

(Received 3 February 1998; accepted 12 May 1998)

We present a new algorithm for Reverse Monte Carlo (RMC) simulations of liquids. During the simulations, we calculate energy, excess chemical potentials, bond-angle distributions and three-body correlations. This allows us to test the quality and physical meaning of RMC-generated results and its limitations. It also indicates the possibility to explore orientational correlations from simple scattering experiments. The new technique has been applied to bulk hard-sphere and Lennard-Jones systems and compared to standard Metropolis Monte Carlo results. © 1998 American Institute of Physics. [S0021-9606(98)50731-3]

I. INTRODUCTION

The Reverse Monte Carlo (RMC) technique¹⁻⁶ has emerged as a tool for determining the structure of liquids and glasses.^{2,3} The experimentally determined radial distribution functions (rdfs), or structure factors, are used as input in the simulation. The particles of the simulated system are then displaced using a Monte Carlo (MC) procedure to generate configurations that correspond to the input (experimental) rdf. During the simulation other structural information may be collected. In recent years, a number of applications of the RMC technique to atomic and molecular systems has appeared.¹⁻⁸ RMC is appealing in that various other sources of information may be taken advantage of. For instance, knowledge in terms of bond lengths, bond angles, coordination numbers and distance constraints may be used in the simulation to complement the input data. However, while the RMC simulation generates many-body correlations there is a question of how relevant they are to the experimental system. The aim of this work is to present a detailed analysis of the three-body correlation functions generated by Metropolis Monte Carlo (MMC) and RMC. In addition, we describe a new RMC algorithm with improved convergence properties.

We will focus on bulk fluids of spherical particles with interactions given by pairwise additive central forces. Evans⁹ noted that for such a system, the pair potential, and therefore all higher ordered distribution functions, are determined by the rdf. To confirm that the RMC technique generates the correct three-dimensional structure, a simple numerical test was proposed. First, a conventional MMC simulation is carried out and the generated rdf is used as input in an RMC simulation. The three-body correlation functions obtained by the two simulations are then compared. Previous studies along this route have focused on the comparison of the so called bond angle and coordination distribution functions.^{2,4,7,8} As we will show, however, these are not suitable for a critical comparison. Instead, the deviations from the Kirkwood superposition approximation¹⁰ at the three particle level appear more useful for a careful examination.

A number of more or less serious convergence difficulties have been reported for the RMC technique. In general it seems that better convergence is obtained with simulations using large system sizes, typically on the order of several thousand particles.^{2,6} In difficult cases, annealing procedures have been proposed as a way to improve convergence and avoid getting trapped into local minima. Another feature of the algorithm used is that large errors are obtained in regions of short distances. Thus, at small particle separations, impenetrable hard-core conditions are introduced to exclude configurations with too close encounters.^{6,8} Some of this may be of little consequence in practical applications, as the experimentally determined distribution functions inevitably contain various sources of errors which may lead to inconsistencies. Thus, one has to allow for some difference between the input and generated structure. In theoretical tests, however, it should be important to obtain as good an agreement as possible. In this work, we will present a modified algorithm which gives excellent convergence even for short distances, and it allows one to avoid the introduction of *ad hoc* hard-core constraints.

Comparisons between the different simulation techniques are almost entirely based on structural data. For molecular systems in particular, such tests may be quite involved.¹¹ As a simple complement we suggest the use of thermodynamic functions as well, e.g., configurational energy and excess chemical potentials. The latter is an important bulk property which implicitly contains contributions from the higher order distribution functions. Armed with these tests, one can investigate if the RMC results have a physical meaning.

As model systems we will use bulk hard-sphere and Lennard-Jones fluids. At first, the new algorithm and its convergence properties are presented. This is followed by comparisons of the energy and excess chemical potentials. Finally, an analysis of various three-body correlation functions is made.

II. A NEW RMC ALGORITHM

The new RMC algorithm that we propose here follows the original idea.¹ The principle is to generate a set of con-

^{a)}Also affiliated with Departamento de Química, Fac. de Ciências, Universidade Estadual Paulista, Unesp 17033-360 Bauru, SP, Brazil.

figurations which corresponds to an input radial distribution function or structure factor. Instead of trying to minimize the free energy like MMC,^{12,13} we minimize the difference between the calculated and experimental rdf. The following notation is used: $g_e(r)$ is the experimental (input) rdf, $g_s(r)$ is the simulated one, and $g_a(r)$ the final answer, the corresponding histograms used to create these rdfs will appear with the same subscript— $\text{hist}_s(r)$ and $\text{hist}_a(r)$. We can summarize our procedure as follows:

- (1) As in “traditional” simulations, we start with an initial configuration of particles in a cubic box. This configuration could be either generated from random coordinates or starting from a lattice. It is of importance that the density is the same as in the experimental system being studied. Usual periodic boundary conditions are applied in all directions. To determine the atomic separations, the minimum image convention is assumed. At this stage, we check the distances and build the histogram, $\text{hist}_s(r)$, which contains the number of atoms at a distance between r and $r + \Delta r$ from a central atom. The number of observations, n_{obs} , is equal to $N - 1$, where N is the number of atoms. We duplicate $\text{hist}_s(r)$ in two other histograms, $\text{hist}_{s_{\text{new}}}(r)$ and $\text{hist}_{s_{\text{old}}}(r)$.
- (2) We attempt single particle random displacements as in standard MMC.^{12,13} Using the new configuration, we recalculate the distances and add the new observation to $\text{hist}_{s_{\text{new}}}(r)$. The original (old) distances are added to $\text{hist}_{s_{\text{old}}}(r)$. Two trial rdfs are calculated as,

$$g_{s_{\text{new}}}(r) = \frac{\text{hist}_{s_{\text{new}}}(r)}{n_{\text{obs}} 4\pi r^2 \Delta r \rho} \quad (1)$$

and

$$g_{s_{\text{old}}}(r) = \frac{\text{hist}_{s_{\text{old}}}(r)}{n_{\text{obs}} 4\pi r^2 \Delta r \rho}, \quad (2)$$

where ρ is the number density of the system. It should be noticed that both $\text{hist}_{s_{\text{new}}}(r)$ and $\text{hist}_{s_{\text{old}}}(r)$ are based on accumulative distance observations since the simulation beginning, and contain the same number of observations.

- (3) These are compared to the experimental $g_e(r)$,

$$\chi_{\text{new}}^2 = \sum_{i=1}^{nl} [g_{s_{\text{new}}}(r_i) - g_e(r_i)]^2 \quad (3)$$

and

$$\chi_{\text{old}}^2 = \sum_{i=1}^{nl} [g_{s_{\text{old}}}(r_i) - g_e(r_i)]^2, \quad (4)$$

where nl is the number of points in the experimental $g_e(r_i)$. The new configuration is accepted if $\chi_{\text{new}}^2 \leq \chi_{\text{old}}^2$. This algorithm is similar to one previously described by Kaplow *et al.*¹⁴ It might be useful to note that, for polyatomic systems, the χ^2 equation could be rewritten in a more convenient form,^{1,2} which allows one to adopt different weights for each intermolecular rdf.

- (4) If the new configuration is accepted, the histogram $\text{hist}_s(r)$ assumes the value of $\text{hist}_{s_{\text{new}}}(r)$ and the coordinates are updated. Otherwise, the old configuration is retained and $\text{hist}_s(r)$ receives $\text{hist}_{s_{\text{old}}}(r)$. Then, n_{obs} is

increased by one, a new particle will be displaced and the process will be repeated from step 2. This action should be repeated until χ^2 decreases and oscillates around a constant value. One critical test of the simulation is the inspection on the histogram, where hard-core overlaps should be absent. So far, we made all comparisons in terms of rdf but this could be easily exchanged for the structure factors.

- (5) It is only the configurations generated during the production phase from which properties of the system are calculated, as, for instance, the average chemical potential. The rdf used in the Markov chain is, however, obtained by a further accumulation of the results from step 4. The present RMC algorithm will usually need more steps to give statistically independent configurations than MMC. Compared to the conventional RMC algorithm,^{1,2} the main differences are: (a) the use of a pure minimization criterion on the present version, and (b) the manner in which the hard-core region is handled. Here, this is done by the employment of accumulative distance observations to produce the rdf, which has also the benefit of requiring a smaller number of particles. In previous works, a hard-core constraint was explicitly introduced.² Another alternative is to introduce a “relative error” for the χ^2 parameter, i.e.,

$$\chi_{\text{new}}^2 = \sum_{i=1}^{nl} \frac{[g_{s_{\text{new}}}(r_i) - g_e(r_i)]^2}{g_e(r_i)} \quad (5)$$

and

$$\chi_{\text{old}}^2 = \sum_{i=1}^{nl} \frac{[g_{s_{\text{old}}}(r_i) - g_e(r_i)]^2}{g_e(r_i)}, \quad (6)$$

which gives almost identical results in our tests. Obviously, in this approach hard-core overlaps are avoided in a straightforward way.

III. MODEL SYSTEMS

As an illustration of the new algorithm, we explored hard-sphere (HS) and Lennard-Jones (LJ) fluids. Both MMC and RMC simulations were carried out for several systems with a small number of particles ($N = 256$). During the production phase, we applied the Widom’s test particle technique¹⁵ to calculate the excess chemical potential (μ^{exc}) for the generated configurations. It should be stressed that in RMC μ^{exc} was calculated assuming that the collected configuration interacted with the test particle according to the pair potential. The pair potential was used only for analysis purposes. In our studies, the input rdf was generated by an equivalent MMC simulation. The displacement parameter was chosen to give 50% of acceptance for MMC experiments, although for RMC we found better convergence with $\sim 40\%$ of acceptance. It seems for our limited experience that RMC is more sensitive to the displacement parameter. Equilibration runs with 10^3 , and $5 \cdot 10^3$ cycles were performed for the MMC and RMC, respectively. The volume fraction was in the range of $\eta = 0.05$ to 0.3 , see Table I.

A set of LJ systems with different densities was studied. MMC and RMC simulations were carried out for reduced densities $\rho^* = \rho \sigma^3$ ranging from 0.1 to 0.8 . We assumed a

TABLE I. Summary of HS runs performed, all with $N=256$ particles. The standard deviation was obtained from a subdivision of the production run into ten parts.

System	η	$\mu_{\text{MMC}}^{\text{exc}}$	$\mu_{\text{RMC}}^{\text{exc}}$
1	0.05	0.434(12)	0.441(2)
2	0.10	0.987(16)	0.976(2)
3	0.15	1.643(22)	1.645(5)
4	0.20	2.483(38)	2.483(9)
5	0.2205	2.879(73)	2.882(12)
6	0.25	3.519(61)	3.554(22)
7	0.276	4.274(115)	4.208(24)
8	0.30	4.914(208)	4.894(58)

cutoff at half ($L/2$) of the cubic simulation box ($V=L^3$) and a tail correction term was applied to correct the configurational energy and the chemical potential.^{13,16} The reduced temperature was fixed at $T^*=kT/\epsilon=1.2$, which is below the liquid-gas critical temperature. Like in the HS case, the number of particles was small, compared to previous studies.² The acceptance control was the same as described before and the simulation lengths were 10^4 cycles. The U and μ^{exc} results presented here were obtained assuming that the RMC-generated configurations obeyed the same LJ potential as used in the MMC simulation. The data are summarized in Table II. We also simulated a system with a slightly higher temperature $T^*=1.58$ and reduced density $\rho^*=0.65$ to allow a comparison with three-body correlations of previous studies.¹⁷

IV. RESULTS AND DISCUSSION

A. Radial distribution function

In Fig. 1, we present typical rdfs obtained by our RMC algorithm and compare them with MMC simulations. It is clear that the structure is well reproduced for both HS [Figs. 1(a) and 1(b)] and LJ fluids [Figs. 1(c) and 1(d)] at low as well as at high densities. In fact, it is only possible to see the differences between the MMC and RMC data if we plot the MMC minus the RMC rdf. The difference is on the order of 10^{-4} – 10^{-5} and even smaller than what one would obtain by two distinct MMC runs. It is important to notice that our algorithm gives excellent convergence without the use of *ad hoc* hard-core constraints. Even with the hard-core constraint, other RMC simulations seem to have a worse agree-

ment than presented here.² In some simulations, systems as large as 4000 LJ particles show distortions in the rdf close to the first peak.²

B. Energy and chemical potential

Configurations collected during the runs were the subject of energy analyses, which is one way to assure that we obtained an appropriate sampling of configurations. Table II shows the outcome of our MMC and RMC simulations together with MC simulations of Ding and Valleau.¹⁶ The two MMC results are within estimated errors and the agreement between our RMC and MMC calculations is surprisingly good, with a relative error of $\sim 2.0\%$. This difference could be made smaller by decreasing the bin size (Δr) used to build the histograms. In all runs presented in Table II, we adopt $\Delta r=0.05$, and Table III lists results for RMC calculations with LJ system 6 ($\rho^*=0.60$) and varying Δr . As stated above, a smaller Δr brings the RMC results closer to the MC ones. For instance, with $\Delta r=0.01$ the error is less than 0.1%.

The chemical potential is not sensitive to changes in Δr . Tables I and II show that μ^{exc} from MMC and RMC is in good agreement and for the studied HS systems our RMC results and MMC are within statistical errors. For the LJ systems, our numbers are close to the results of Ding and Valleau.¹⁶ The test particle method shows a decreasing of efficiency as the density increases. See Fig. 2.

C. Three-body correlations

Several simulation studies of one component monoatomic systems have been made in order to compare the three particle correlations obtained with MC and RMC^{2,4,7} and thereby to verify Evans' proof.⁹ To a large extent the comparisons have relied upon analyses of what has been termed the "bond-angle" (which does not refer to a true chemical bond) distribution function, $b(\theta)$, and the coordination number distribution function, $P(n)$. Given that a particle has more than one neighbor within a cutoff distance, r_c , $b(\theta)d\theta$ is the probability for the position vectors of the neighbors relative to the central atom to form an angle between θ and $\theta+d\theta$. However, as we will show below, this function by itself is not particularly useful in making a critical comparison on three-body correlations generated by the two simulation techniques. $P(n)$ is the probability of observ-

TABLE II. Summary of LJ runs performed with $N=256$ particles. The unit for U and μ^{exc} are NkT and kT , respectively. U_{Valleau} and $\mu_{\text{Valleau}}^{\text{exc}}$ were taken from Ref. 16. The standard deviation was obtained from a subdivision of the production run into 20 parts.

System	ρ^*	$-U_{\text{RMC}}$	$-U_{\text{MMC}}$	$-U_{\text{Valleau}}$	$-\mu_{\text{RMC}}^{\text{exc}}$	$-\mu_{\text{MMC}}^{\text{exc}}$	$-\mu_{\text{Valleau}}^{\text{exc}}$
1	0.1	0.6925(1)	0.700(2)	...	0.726(2)	0.722(2)	...
2	0.2	1.3406(1)	1.356(8)	1.358(12)	1.340(3)	1.327(3)	1.325(7)
3	0.3	1.8850(1)	1.908(7)	1.898(12)	1.825(6)	1.808(4)	1.814(15)
4	0.4	2.3560(2)	2.386(9)	2.388(7)	2.199(6)	2.199(8)	2.191(10)
5	0.5	2.8403(2)	2.879(3)	2.882(5)	2.442(10)	2.443(8)	2.432(17)
6	0.6	3.3667(2)	3.418(2)	3.417(2)	2.442(15)	2.431(16)	2.447(16)
7	0.7	3.8920(2)	3.963(1)	3.965(2)	2.014(25)	1.975(31)	1.946(52)
8	0.8	4.3677(3)	4.468(2)	4.473(4)	0.609(113)	0.564(100)	0.687(136)

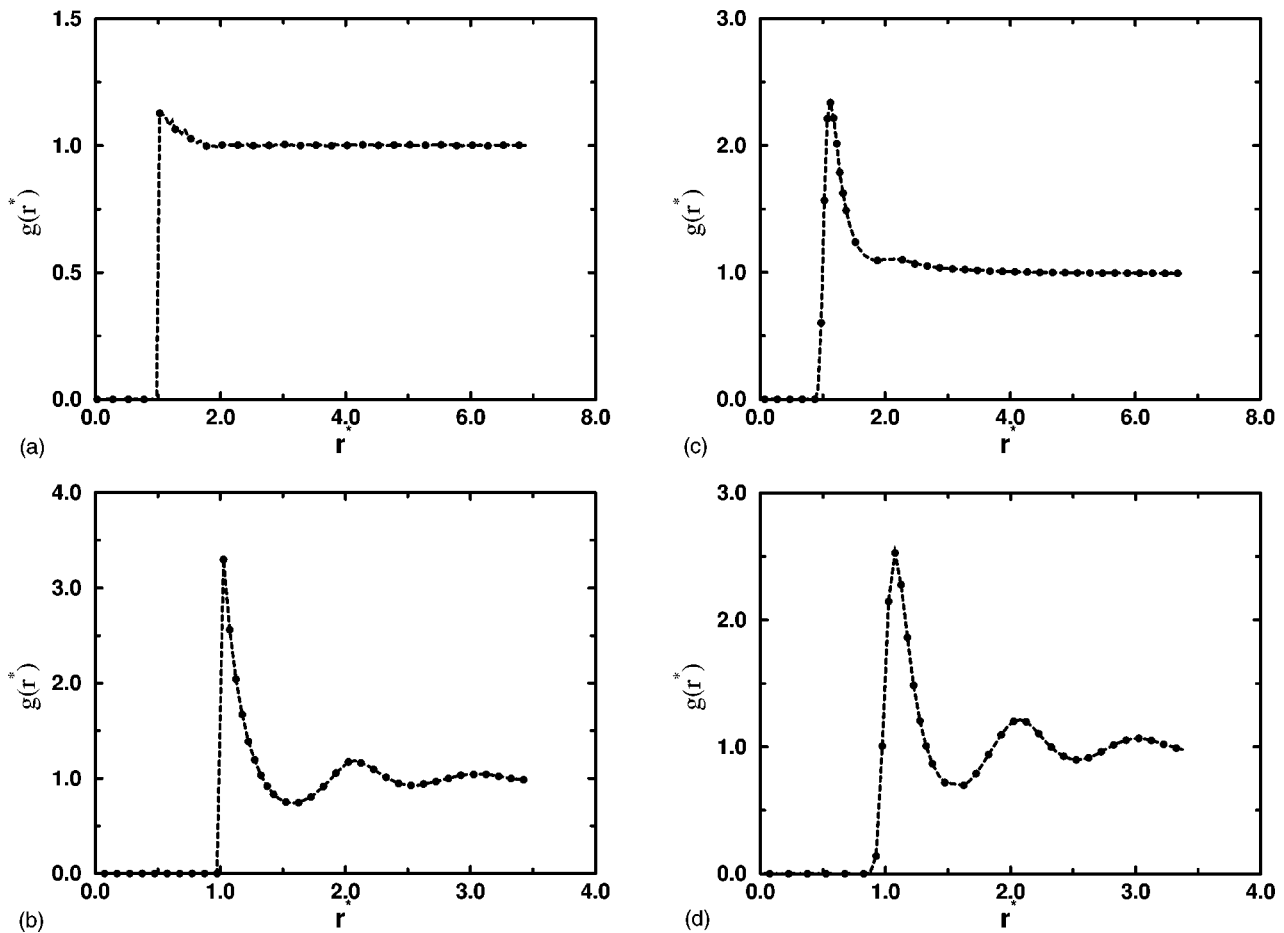


FIG. 1. Comparison between experimental (---) rdf and RMC (●). HS system at (a) low density ($\eta=0.05$) and (b) at high density ($\eta=0.4$); LJ system at (c) low density ($\rho^*=0.1$) and (d) at high density ($\rho^*=0.8$) with reduced temperature at $T^*=1.2$. Reduced units are used in this graph and in all the following ones, meaning $r^*=r/\sigma$, $\rho^*=\rho\sigma^3$, $T^*=kT/\epsilon$, and $\mu^*=\mu/kT$.

ing n particles within a specified distance from a central particle. For reasons which will be obvious later, it seems that this function is not suited as a critical test.

Writing the $b(\theta)$ function in terms of the radial distribution function at the three particle level, $g^{(3)}(r_{12}, r_{13}, r_{23})$, one has

$$b(\theta) = \int_0^{r_c} \int_0^{r_c} dr_{12} dr_{13} g^{(3)}(r_{12}, r_{13}, (r_{12}^2 + r_{13}^2 - 2r_{12}r_{13} \cos \theta)^{1/2}) r_{12}^2 r_{13} \sin \theta, \quad (7)$$

where a normalization constant has been left out. For convenience we introduce the correlation function δ_{123} given by

$$\delta_{123}(r_{12}, r_{13}, r_{23}) = \frac{g^{(3)}(r_{12}, r_{13}, r_{23})}{g(r_{12})g(r_{13})g(r_{23})}. \quad (8)$$

This function gives the deviation from the superposition approximation,¹⁰ which in turn will depend on the pair inter-

TABLE III. Influence of the bin size, Δr , for the LJ system 6. U and μ^{exc} are given in NkT and kT units, respectively.

Δr	$-U_{\text{MMC}}$	$-U_{\text{RMC}}$	$-\mu_{\text{MMC}}^{\text{exc}}$	$-\mu_{\text{RMC}}^{\text{exc}}$
0.050	3.418(2)	3.3665(2)	2.431(16)	2.448(10)
0.030	...	3.3910(9)	...	2.442(10)
0.025	...	3.4059(1)	...	2.418(10)
0.020	...	3.4103(1)	...	2.418(11)
0.010	...	3.4161(2)	...	2.414(11)

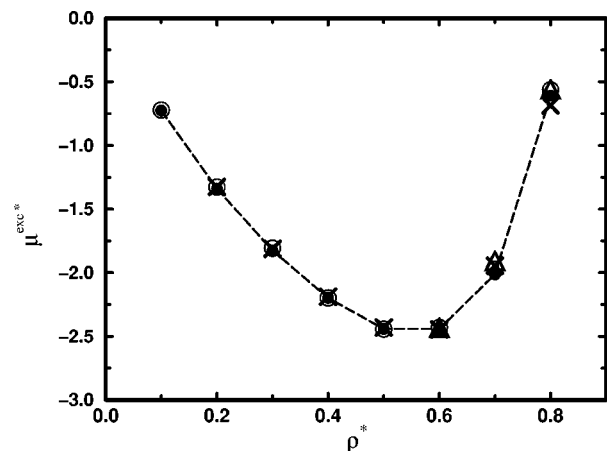


FIG. 2. The μ^{exc} in kT units as a function of the density for LJ system. (●) RMC, (○) MMC, (×) Ding and Valleau (Ref. 16) and (△) Smit and Frenkel's (Ref. 19).

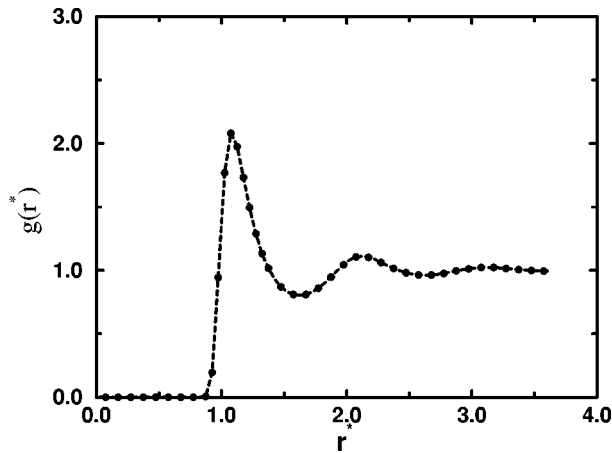
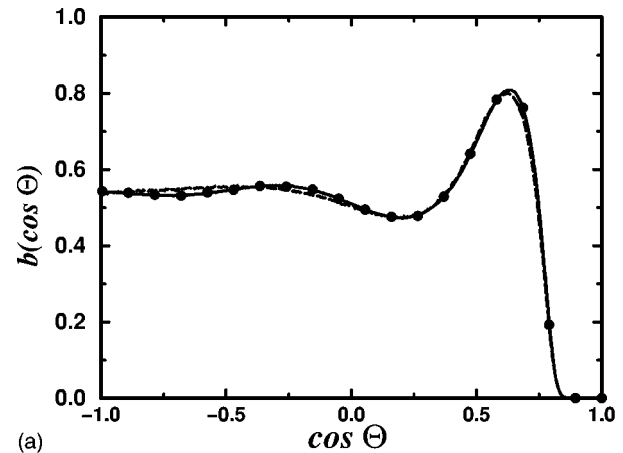


FIG. 3. MMC (---) and RMC (●) rdf for a LJ system at reduced density $\rho^*=0.65$ and temperature $T^*=1.56$.

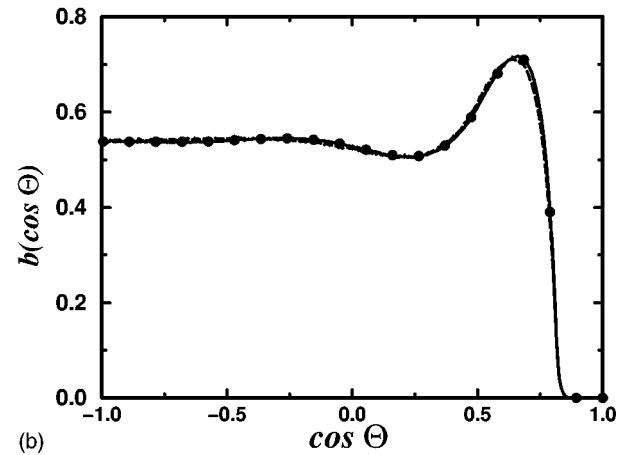
action, density and the separations between the three particles. For any system with pair interactions, δ_{123} will approach unity as the separation between two of the particles becomes large. It is clear that if the superposition approximation is accurate at all separations for the particular system under study, the agreement between the $b(\theta)$ functions obtained by MMC and RMC becomes trivial. However, there are further weaknesses in using this function as a probe of the three-body correlation functions. Even if δ_{123} deviates from one, the dominating contribution to $b(\theta)$ comes from the larger separations where, depending on the cutoff value (r_c), δ_{123} may be close to unity. There is also a possibility that the integration will cancel the contributions from regions which may have positive or negative deviations from the superposition approximation.

As an illustration we reinvestigate a LJ system recently described in the literature.² We performed our simulation with data described before (LJ system 9), although the referenced one has a slightly higher density ($\rho^*=0.67$). This difference is not significant for our purposes and our system has the further advantage to be directly comparable to another three-body correlation work.¹⁷ Figure 3 shows the rdf with 256 LJ particles. In Fig. 4(a) we compare $b(\theta)$ obtained using a MMC, RMC and the superposition approximation with a cutoff distance equal to the position of the first minimum in the rdf, $r_c=1.625\sigma$. The excellent agreement between RMC and MMC is seen to be trivial in this case as the superposition approximation gives an almost equally good result. A more convincing example is given in Fig. 4(b), for a HS system with a packing fraction of 0.276. It is expected that HS usually shows less deviations from the superposition approximation and so the agreement with MMC and RMC is even closer.

It seems natural then that a first criterion for a critical structural comparison between MMC and RMC has to be made on a system which shows deviations from the superposition approximation. To make the test sensitive, we suggest that it is based on a comparison of the δ_{123} function itself, and furthermore the function should not be integrated over large volumes where its structure may be lost. We have made such analyses for the LJ system 9. In Fig. 5, the δ_{123}



(a)



(b)

FIG. 4. Bond-angle distribution for (a) LJ system at $\rho^*=0.65$, $T^*=1.56$ and $r_c=1.625\sigma$, and (b) HS system at $\eta=0.276$ and $r_c=1.725\sigma$. For both cases, r_c corresponds to the first rdf minimum. MMC (—), RMC (●) and the superposition approximation (---) data.

function is shown as a function of the distance at an isosceles fixed particle separation. Within the statistical fluctuations we obtain the same deviation from unity in both MMC and RMC. RMC results tend to underestimate δ_{123} function only at very short distances. It is probably a confirmation that RMC tends to generate a more disordered structure as sug-

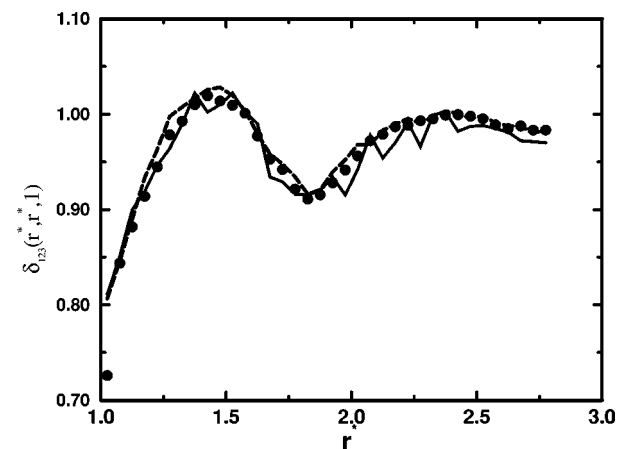


FIG. 5. The $\delta_{123}(r_{12}, r_{13}, r_{23})$ function for LJ particles ($\rho^*=0.65$ and $T^*=1.56$) at different isosceles configurations with $r_{12}=r_{13}$ and r_{23} fixed at $1.025/\sigma$. RMC (●), MMC (---) and Ravechè *et al.* (—) (Ref. 17).

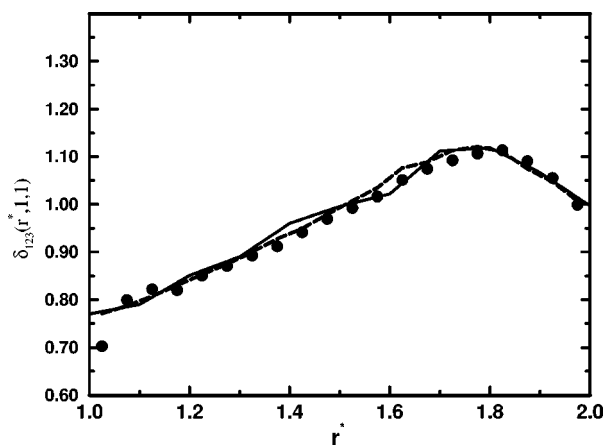


FIG. 6. The $\delta_{123}(r_{12}, r_{13}, r_{23})$ function for a HS system ($\eta=0.276$) at isosceles configurations with both r_{13} and r_{23} fixed at $1.025/\sigma$. RMC (●), MMC (---) and Uehara *et al.* (—) (Ref. 18).

gested before.² It is clearly seen that the δ_{123} function approaches unity with increasing of distance. Our results are also close to the data of Raveché *et al.*¹⁷

We extend our study to the previously investigated HS systems, at a packing fraction of 0.276.¹⁸ Figure 6 shows δ_{123} as a function of the particle separation and at an isosceles fixed particle distance. Again, RMC seems to slightly underestimate δ_{123} close to contact. The $g^{(3)}(r_{12}, r_{13}, r_{23})$ function is found to be well reproduced and confirms that, if the pair potential is additive, then RMC generates configurations with satisfactory three-body correlation properties. As far as we are aware, this is the first convincing numerical test of Evans' proof.⁹

It may be worthwhile to here also make some technical comments on the analyses of $b(\theta)$ for systems with oscillations in $g(r)$ extending out to separations larger than half the box length. Using r_c values larger than a quarter of the box length will then at large θ introduce various sources of errors in the $b(\theta)$ function. First, RMC is not optimized to give correct structures at separations larger than half the box length, which means that the rdf in the "corners" of the box may be different than that given by MMC. Second, an artificial structure is introduced by including contributions from particles beyond the minimum image. This may explain the extremely large finite size effects obtained in some systems.⁷

We now return to the suitability of the coordination number distribution function for structural comparisons between the two simulation techniques. The mean coordination number is given by the rdf and must therefore be correctly reproduced by a successful RMC simulation. However, $P(n)$ is given by higher order correlation functions. This, together with the fact that it is easy to calculate in a simulation, has made it popular for structural comparisons between MC and RMC.^{2,4} The coordination number distribution function may, with increasing accuracy, be approximated by spatial averages of two, three and higher order correlation function. A critical test between MMC and RMC has to show that the

rdf, together with the superposition approximation, does not reproduce $P(n)$. As far as we are aware, this has never been done. Thus, a simple comparison of $P(n)$ obtained with the two techniques gives limited information regarding the quality of the many-body correlation functions generated by RMC.

V. CONCLUSION

We present a new algorithm with improved convergence properties for reversed Monte Carlo simulations. The RMC technique has been investigated using thermodynamic and structural analyses. The agreement between the input and generated rdfs was impressive, even though system sizes were very small and no hard-core constraints were imposed. It was shown that bond-angle distribution functions and coordination number distribution function are of little value in proving the accuracy of the higher order correlation functions generated by RMC. Instead, it was argued that sensitive tests should be based on functions, which clearly show deviation from Kirkwood's superposition approximation. The RMC-generated configurations produced similar configurational energy and excess chemical potential as the MMC simulations. It seems that this version can be easily extended to other molecular liquids and can provide an extra tool for liquid crystallography studies.

ACKNOWLEDGMENTS

This work has been supported by the *Conselho Nacional de Desenvolvimento Científico e Tecnológico* (CNPq/Brazil), whom F.L.B.D.S. wishes to thank. It is also a pleasure to acknowledge Léo Degrève and Wilmer Olivares for several discussions and *Cenapad* (CNPq/Brazil) for computational support.

- ¹R. L. McGreevy and L. Pusztai, *Mol. Simul.* **1**, 369 (1988).
- ²R. L. McGreevy and M. A. Howe, *Phys. Chem. Liq.* **24**, 1 (1991).
- ³R. L. McGreevy and M. A. Howe, *Annu. Rev. Mater. Sci.* **22**, 217 (1992).
- ⁴A. Shick and R. Rajagopalan, *Colloids Surface* **66**, 113 (1992).
- ⁵I. Bakó, P. Jedlovsky, and G. Pálinkás, *Chem. Phys. Lett.* **221**, 183 (1994).
- ⁶M. A. Howe, R. L. McGreevy, and J. D. Wicks, *RMCA—A General Purpose Reverse Monte Carlo Code* (Manual, 1993).
- ⁷L. Pusztai and G. Tóth, *J. Chem. Phys.* **94**, 3042 (1991).
- ⁸L. Pusztai, M. A. Howe, R. L. McGreevy, and I. Borszak, *Phys. Chem. Liq.* **25**, 205 (1993).
- ⁹R. Evans, *Mol. Simul.* **4**, 409 (1990).
- ¹⁰J. G. Kirkwood, *J. Chem. Phys.* **20**, 929 (1952).
- ¹¹H. Xu and M. Kotbi, *Chem. Phys. Lett.* **248**, 89 (1996).
- ¹²N. A. Metropolis, A. W. Rosenbluth, M. N. Rosenbluth, A. Teller, and E. Teller, *J. Chem. Phys.* **21**, 1087 (1953).
- ¹³M. P. Allen and D. J. Tildesley, *Computer Simulation of Liquids* (Oxford University Press, Oxford, 1989).
- ¹⁴T. A. Rowe, R. Kaplow, and B. L. Averbach, *Phys. Rev.* **168**, 1068 (1968).
- ¹⁵B. Widom, *J. Chem. Phys.* **39**, 2808 (1963).
- ¹⁶K. Ding and J. P. Valleau, *J. Chem. Phys.* **98**, 3306 (1993).
- ¹⁷R. D. Mountain, H. J. Raveché, and W. B. Street, *J. Chem. Phys.* **57**, 4999 (1972).
- ¹⁸T. Ree, Y. Uehara, Y. T. Lee, and F. H. Ree, *J. Chem. Phys.* **70**, 1884 (1979).
- ¹⁹B. Smit and D. Frenkel, *J. Phys.: Condens. Matter* **1**, 8659 (1989).